Glycyrrhizic acid induces human MDA-MB-231 breast cancer cell death and autophagy via the ROS-mitochondrial pathway

SHU-CHUAN LIN[1,2], PEI-YI CHU[3-5], WAN-TING LIAO[6,7], MENG-YU WU[8,9], KUAN-HAO TSUI[10-12], LI-TE LIN[10,11], CHIH-HAO HUANG[13,14], LI-LI CHEN[15,16] and CHIA-JUNG LI[17]

[1]Department of Public Health, China Medical University, Taichung 404; Departments of [2]Nursing and [3]Pathology, Show Chwan Memorial Hospital, Changhua 500; [4]School of Medicine, College of Medicine, Fu Jen Catholic University, New Taipei City 242; [5]National Institute of Cancer Research, National Health Research Institutes, Tainan 704; [6]Chinese Medicine Department, Show Chwan Memorial Hospital, Changhua 500; [7]Graduate Institute of Chinese Medicine, School of Chinese Medicine, China Medical University, Taichung 242; [8]Department of Emergency Medicine, Taipei Tzu Chi Hospital, Buddhist Tzu Chi Medical Foundation, New Taipei 231; [9]Department of Emergency Medicine, School of Medicine, Tzu Chi University, Hualien 970; [10]Department of Obstetrics and Gynecology, Kaohsiung Veterans General Hospital, Kaohsiung 813; [11]Department of Obstetrics and Gynecology, National Yang-Ming University School of Medicine, Taipei 112; [12]Department of Pharmacy and Master Program, College of Pharmacy and Health Care, Tajen University, Pingtung County 907; [13]Institute of Biotechnology, National Changhua University of Education; [14]Laboratory of Animal Center, Department of Medical Research and Development, Show Chwan Health Care System, Changhua 500; [15]School of Nursing, College of Health Care, China Medical University and [16]Department of Nursing, China Medical University Hospital, Taichung 404; [17]Research Assistant Center, Show Chwan Memorial Hospital, Changhua 500, Taiwan, R.O.C.

Received June 12, 2017; Accepted November 17, 2017

DOI: 10.3892/or.2017.6123

Abstract. Glycyrrhizic acid (GA), the main component of licorice root extracts, has been shown to suppress cell proliferation and induce apoptosis in various types of cancers. However, the molecular mechanism of its anticancer activity remains poorly understood and warrants further investigation. MDA-MB-231 cells were treated with various concentrations of GA and the cytotoxic effects of GA were determined using the CCK-8 assay. Apoptosis and cell cycle status were detected by flow cytometry. Reactive oxygen species (ROS) levels and mitochondrial membrane potential ($\Delta\Psi m$) were assessed using DCFDA, MitoSOX and JC-1 staining. Western blot analysis was used to quantify the expression of autophagy-related proteins. In the present study, induction of autophagic cell death was observed in GA-treated MDA-MB-231 cells. Downregulation of p62- and beclin 1-associated proteins occurred after GA treatment, and, the conversion of LC3 and increased ROS without significant changes in caspase-associated proteins and intracellular responses were detected. Furthermore, loss of mitochondria and its membrane potential in cells demonstrated that mitochondria were involved in the GA-regulated MDA-MB-231 cell death. The addition of a pan-caspase inhibitor (z-VAD-fmk) did not suppress the GA-induced apoptotic effect, and GA-induced apoptosis was not accompanied by processing of procaspase-8, -9 and -3. However, GA triggered the translocation of the apoptosis-inducing factor (AIF) from the mitochondria into the nucleus. In contrast, GA-induced LC3 conversion was significantly inhibited by 3 methlyadenine (3MA), an inhibitor of PI3K-regulated autophagy. Therefore, these results suggest that enhancement of both AIF- and LC3-dependent GA-derived ROS generation plays an important role in the inhibition of the growth of MDA-MB-231 human breast cancer cells.

Correspondence to: Dr Li-Li Chen, School of Nursing, College of Health Care, China Medical University, 91 Hsueh-Shih Road, North, Taichung 404, Taiwan, R.O.C.
E-mail: lily@mail.cmu.edu.tw

Dr Chia-Jung Li, Research Assistant Center, Show Chwan Memorial Hospital, 542 Section 1, Chung-Shang Road, Changhua, Taiwan, R.O.C.
E-mail: nigel6761@gmail.com

Key words: glycyrrhizic acid, mitochondria, apoptosis-inducing factor, autophagy

Introduction

Breast cancer is highly metastatic, leading to multiorgan dysfunction and a high mortality rate (1,2), which can be reduced by early detection and optimized therapeutic options (3-5). Triple-negative breast cancer (TNBC) is an aggressive subtype that does not respond to estrogen receptor (ER)-, progesterone receptor (PR)- and human epidermal growth factor receptor 2 (HER2)-targeted therapies, and TNBC patient prognoses are poor (6,7). Surgery, radiotherapy, chemotherapy and targeted therapy are the standard treatments for breast

cancer (8,9). However, the side-effects associated with these treatments may include critical alopecia, nephrotoxicity and hepatotoxicity (10,11). Drug resistance in cancers is also a serious impediment to treatment and can undermine therapeutic efficacy (12). Furthermore, target therapeutic agents, such as trastuzumab, lapatinib and the anti-angiogenic drug Avastin have demonstrated indeterminate benefits in clinical settings (13-15). Under these circumstances, development of new drugs is particularly compelling and imperative. Although great efforts have been made to design more powerful drugs for the treatment of breast cancer, the results remain unsatisfactory. In fact, some herbal drugs in alternative medicine have been suggested to be a better choice to improve the current therapeutic strategy.

Glycyrrhizic acid (GA) is the main component of licorice root extracts. GA contains 8 hydroxyl groups and is highly hydrophilic; therefore, it is water-soluble and is easily absorbed and metabolized by the digestive tract. GA constitutes ~2-24% of the dry weight of licorice root. Licorice root extracts are sweet, and GA is ~50 times sweeter than sucrose. Therefore, GA is widely used as an additive in candy and food; it is also used in medicine and in the beer manufacturing industry (16). GA was recently demonstrated to induce the apoptosis of human endometrial cancer cells, and potently inhibited the growth of lung cancer cells via caspase activation (17). Previous studies indicate that a mass of compounds induce autophagy for cell death by various mechanisms (18-21), e.g. glycyrrhetinic acid induces autophagy in leukemia and myeloma cells by suppression of the mTOR pathway (22). However, the potential therapeutic effects of GA on mechanisms associated with autophagy have not yet been explored in breast cancer.

Mounting evidence indicates that GA-induced cell apoptosis may be regulated by the caspase cascade in various types of cancers (23-26). However, few studies have specifically focused on GA-induced autophagy, particularly in breast cancer cells (27,28). In the present study, we investigated the effects of GA on mitochondrial cell death in a highly aggressive MDA-MB-231 breast cancer model to determine whether GA provides dual inhibition by enhancing apoptosis and autophagy caused by damaged mitochondria.

Materials and methods

Materials. GA, *N*-acetyl-cysteine (NAC), staurosporine (STS), hydrogen peroxide (H_2O_2), *N*-phenylmaleimide (NPM), 3 methyladenine (3MA), JC-1 and anti-β-actin (A5411) were purchased from Sigma Co. (St. Louis, MO, USA). Anti-AIF (113306), anti-BAX (109683), anti-BCL2 (100064), anti-PARP1 (100573), anti-porin (114187), anti-histone (122148) and z-VAD-FMK were purchased from GeneTex (ICON-GeneTex Inc., Taipei, Taiwan); anti-caspase-8 (ab138485), caspase-9 (ab115161), anti-caspase-3 (ab90437), anti-LC3 (ab48394), anti-beclin 1 (ab62557) and anti-P62 (ab155686) were purchased from Abcam (Cambridge, UK).

Cell culture. MDA-MB-231 human breast carcinoma cell lines were cultured in Dulbecco's modified Eagle's medium (DMEM) (Sigma Co.) supplemented with 10% fetal bovine serum (FBS) (v/v), 100 U/ml penicillin/streptomycin/amphotericin (Sigma Co.) and 0.1 M sodium bicarbonate. Cells were maintained in a humidified incubator at 37˚C with 5% CO_2 and passage by 0.25% trypsin-EDTA every 2-3 days.

Cell proliferation assay. Cell viability was analyzed using Cell Counting Kit-8 (CCK-8) that detects the metabolic activity of cells. At the end of the various treatments, 10 μl of the CCK-8 reagent was added to each well (at $1x10^4$ cells/well), and the cells were then incubated at 37˚C for 4 h. Absorbance was recorded using an ELISA microplate reader at 450 nm.

Cell morphology staining. Cell morphology was studied by Hoechst 33258 and propidium iodide (PI) double staining for live-cell images. After treatment, cells (at $1x10^5$ cells/well) were stained with Hoechst 33258 and PI solution at room temperature for 10 min. Cells were washed twice with phosphate-buffered saline (PBS) for analysis by an inverted fluorescence microscope (Carl Zeiss Axiovert M200; Carl Zeiss, Jena, Germany).

Cell death measurement. Cell survival was assessed by labeling cells with PI. Briefly, the cells (at $1x10^5$ cells/well) were washed twice with PBS, re-suspended in a binding buffer and stained with 1 μg/ml of a PI solution (Sigma Co.) for 15 min at room temperature in the dark. After incubation, the cells were analyzed using flow cytometry.

Cellular production of reactive oxygen species (ROS). Intracellular production of ROS, namely hydrogen peroxide was measured using DCFH-DA (Enzo Life Sciences, Inc., Farmingdale, NY, USA). Cells (at $1x10^5$ cells/well) from each experimental condition were stained with DCFH-DA (2 μM) at 37˚C for 30 min. ROS production of cells was evaluated by flow cytometry (FACSCalibur; Bioscience, Tokyo, Japan). Values were expressed relative to the fluorescence signal of the control.

Mitochondrial function assays. Cells (at $1x10^5$ cells/well) from each experimental condition were stained with JC-1 (10 μg/ml) reagent and MitoSOX Red (Molecular Probes Inc., Eugene, OR, USA) at 37˚C for 30 min for detection of the mitochondrial membrane potential and mitochondrial ROS, respectively. Cells were washed twice with PBS, trypsinized, and collected, and the pellet was re-suspended in PBS for analysis using flow cytometry.

Immunofluorescence labeling and immunoblotting assay. The immunoassay was performed as previously described (28).

Caspase activity. Caspase-8, -9 and -3 activities were measured by the colorimetric activity assay kits (Chemicon International, Temecula, CA, USA). The assay is based on cleavage of the chromogenic substrates, DEVD-pNA and LEHD-pNA, by caspase-3 and -9, respectively. Cells (at $1x10^4$ cells/well) were lysed with the chilled lysis buffer on ice for 10 min and centrifuged for 5 min at 10,000 x g. Supernatant of each treatment was transferred to a fresh tube and equal protein concentration was adjusted to that of the positive control before incubating with the caspase inhibitor in a 96-well microplate for 10 min. Caspase substrate solution with specific peptide substrate was

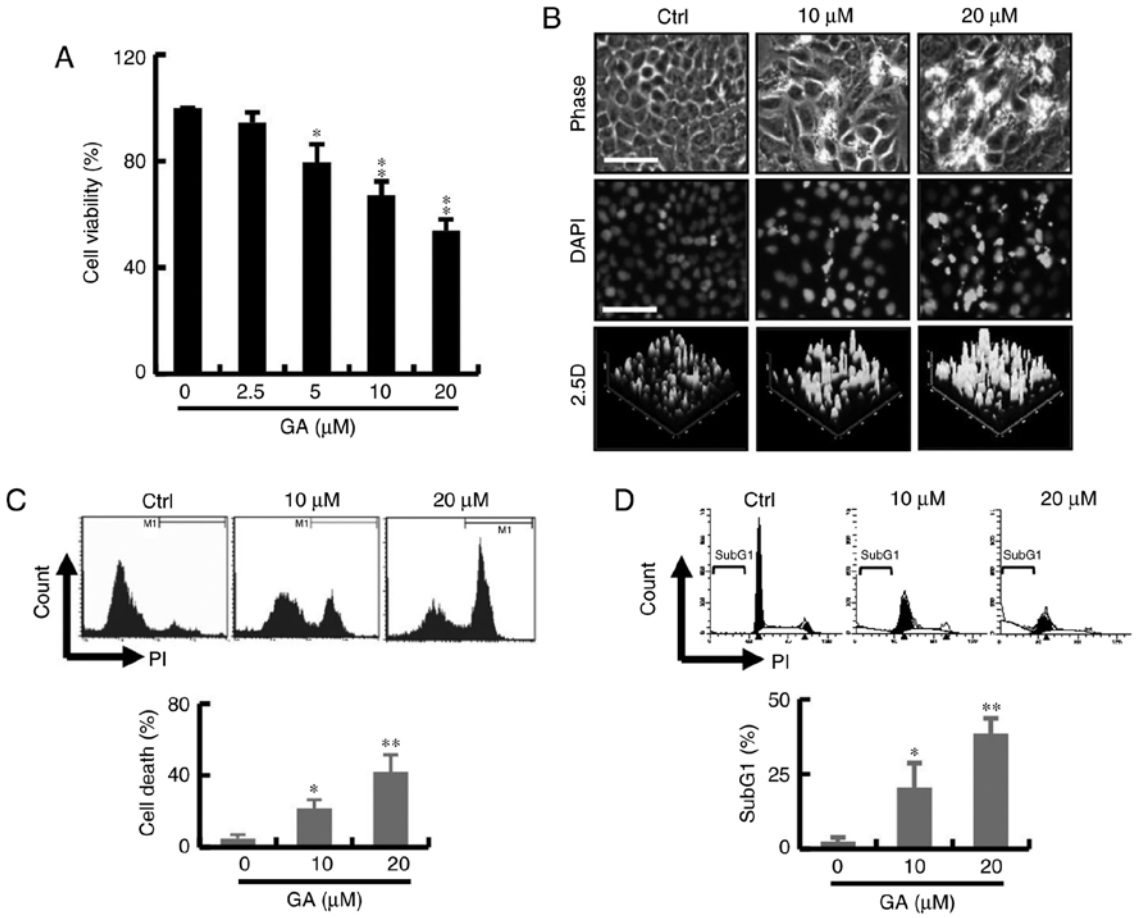

Figure 1. GA exhibits cytotoxic effects, phenotype modification and DNA breakage in breast cancer cells *in vitro*. (A) Cell viability was measured after treatment with 2.5-20 μM GA for 24 h by CCK-8 assay. Each reported value represents the mean ± SEM (*P<0.05; **P<0.01, compared with the untreated control, n=8). (B) DAPI staining for DNA damage. Reconstructed 2.5-dimensional image shows the fluorescence intensity on the surface. Scare bar, 100 μm. (C and D) MDA-MB-231 cells were treated with GA for 24 h and subsequently analyzed using flow cytometry with propidium iodide (PI) staining for live cells and fixed cell to determine the populations exhibiting cell death. Quantitative data were evaluated by the PI-positive population of individual histograms. *P<0.05 and **P<0.01. GA, glycyrrhizic acid.

then added into the supernatant and incubated for 2 h at 37˚C before measuring by ELISA reader at 405 nm.

Cell death detection by Annexin V-FITC/PI double staining. Analysis of the cell death of each condition was performed using an Alexa Fluor Annexin V/Dead Cell Apoptosis kit (Molecular Probes Inc.) according to the manufacturer's protocol. Briefly, cells (at 1x10^5 cells/well) were harvested after treatment. Cells were then washed twice with cold binding buffer, resuspended in binding buffer and stained with 5 μl each of Annexin V-FITC and PI solution for 15 min at room temperature in the dark. After incubation, 1 ml binding buffer was added, and cells were analyzed by flow cytometry.

Statistical analysis. The intensity of bands in western blot analyses or fluorescence was quantified using ImageJ software (NIH) and Zeiss Zen software. The intensity value for each protein was normalized against the intensity of the loading control for that same sample. The values after normalizing to the loading control in the control groups were set as 1.0. Data presented are the mean ± standard error of the mean (SEM) from at least 3 independent experiments and were analyzed using a Student's t-test with two-tailed distribution between groups as indicated in the graphs. All calculations were performed using GraphPad Prism 6.01 version.

Results

Induction of cell death by GA in MDA-MB-231 cells. The effect of GA on cell survival is shown in Fig. 1A. The cytotoxicity of the GA was measured by CCK-8 assay. As shown in Fig. 1A, GA exerted a significant cytotoxic effect at concentrations 2.5-20 mM at 24 h and the IC_{50} value was found to be 20 μM. These results indicated that the GA treatment significantly reduced cancer cell viability in a dose-dependent manner. To further evaluate the cytotoxic effect of GA-induced breast cancer cell death, cells were stained with DAPI after exposure to GA for 24 h. Significant change in blebbing, cell shrinkage, DNA condensation was observed in the MDA-MB-231 breast cancer cells; an increase in fluorescence intensity was observed by 2.5 D reconstruction image after treatment with GA (Fig. 1B). As shown in Fig. 1C, GA markedly increased the percentage of PI-positive cells by live-cell fluorescent. In addition, cell cycle analyses showed an increase in the subG1 phase population at 24 h in the GA treatment groups. The increased subG1 population of GA-treated breast cells at 24 h coincided with that of the cell viability assay (Fig. 1D).

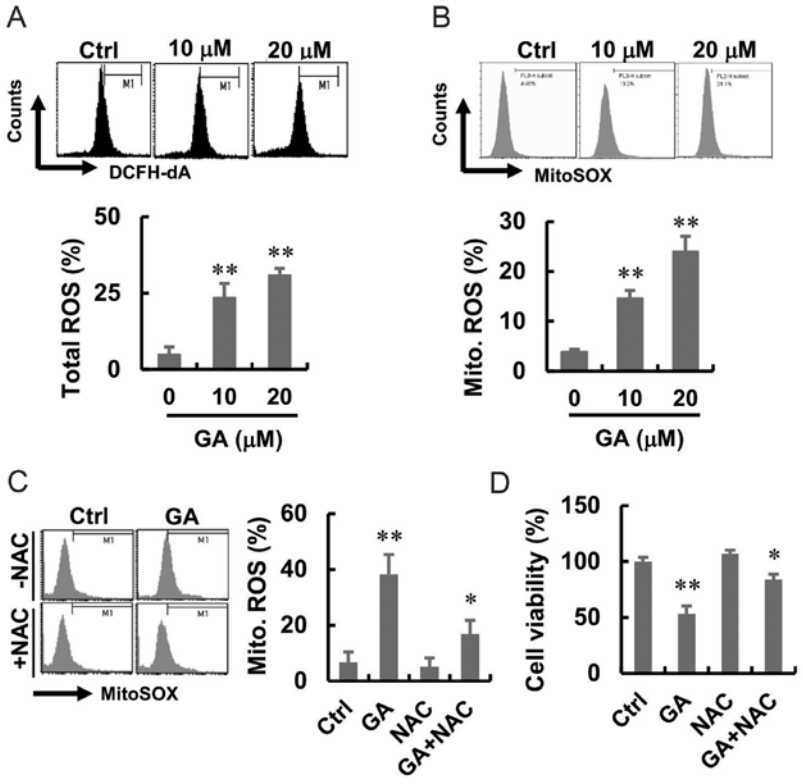

Figure 2. GA increases the generation of intracellular and mitochondrial reactive oxygen species (ROS) in MDA-MB-231 cells. (A and B) Flow cytometric analysis of the intracellular and mitochondrial ROS in various groups of GA-treated cancer cells. Quantitative data were evaluated using the FL1-H and FL2-H of each histogram. The shifts of fluorescence using DCFH-DA and MitoSOX were statistically significant. Vertical lines indicate the mean fluorescence values for the vehicle control cells. (C) Cells were pretreated with NAC (5 mM) for 2 h, followed by GA treatment for 24 h before determination of ROS accumulation by flow cytometry. (D) The survival of MDA-MB-231 cells following GA treatment in the presence or absence of NAC treatment; *P<0.05 and **P<0.01. GA, glycyrrhizic acid; NAC, *N*-acetyl-cysteine.

Treatment with GA significantly elevates the generation of ROS. To investigate the effect of GA on intracellular ROS generation, MDA-MB-231 cells were treated with GA at different concentrations and stained with fluorescent probe DCFH-DA and MitoSOX, which detect hydroperoxide and mitochondrial ROS, respectively. Cells following GA treatment showed higher green and red fluorescence compared with that in the normal control group (Fig. 2A and B). A flow cytometric analysis was performed to quantify the effect of GA-induced intracellular and mitochondrial ROS generation, and the results are presented in Fig. 2A and B. GA induced a significant shift in green and red fluorescence, whereas following GA, enhanced total ROS and mitochondrial ROS production were well apparent. To investigate whether ROS were involved in the GA-induced cell death, we introduced NAC, an inhibitor that blocks ROS generation, before GA treatment. The results showed that NAC alone had no effect on the mitochondrial ROS. However, NAC treatment blocked the GA-induced mitochondrial ROS in MDA-MB-231 cells (Fig. 2C). Moreover, there was increased in cell viability after treatment with GA and NAC (Fig. 2D).

GA induces caspase-independent cell death in MDA-MB-231 cells. Annexin V/PI double-staining was used to detect the PS out-flipping phenomenon, one of the clearest characteristics of apoptotic cell death. To examine whether inhibition of GA-induced cell proliferation was associated with apoptosis, cells were detected after 24 h of GA exposure by flow cytometry. GA reduced the number of viable MDA-MB-231 breast cancer cells from 87 to 60% in a dose-dependent manner. However, we found that the cell population shifted directly to PI^{+} quadrants without going through the PI^{-}/Annexin V^{+} transition. This observation suggests that cell death induced by GA differs from apoptosis in MDA-MB-231 cells, apparently relying mainly on necrosis or autophagy (Fig. 3A). Mitochondrial integrity or the loss of $\Delta\psi m$ has been linked to initiation of apoptosis and multiple cell death, including autophagy and necrosis. To determine $\Delta\psi m$ loss, breast cancer cells were stained with JC-1 when harvested and subjected to flow cytometric analysis. JC-1 concentrates in the mitochondria as red fluorescent aggregates at high membrane potentials and is converted to green monomers when $\Delta\psi m$ is lost. Red fluorescence in MDA-MB-231 breast cancer cells after GA treatment was reduced from 99 to 64%, indicating mitochondrial membrane potential (MMP) depolarization in breast cancer cells (Fig. 3B). To determine whether GA-induced apoptosis, characterized mainly by activation of caspase-3-associated proteins leading to cleavage of PARP1, protein expression was measured by western blotting (Fig. 3C). Along with decreased levels of PARP1 and a significantly increased BAX/BCL2 ratio was observed after GA treatment (Fig. 3D). No changes in cleaved caspase-3, -9 and -8 expression and activity were found in MDA-MB-231 breast cancer cells (Fig. 3C and E). To corroborate that GA-induced cell death was independent of caspase, the cells were pre-treated with 1 mM pan-caspase inhibitor z-VAD-FMK for 2 h. No significant recovery in cell

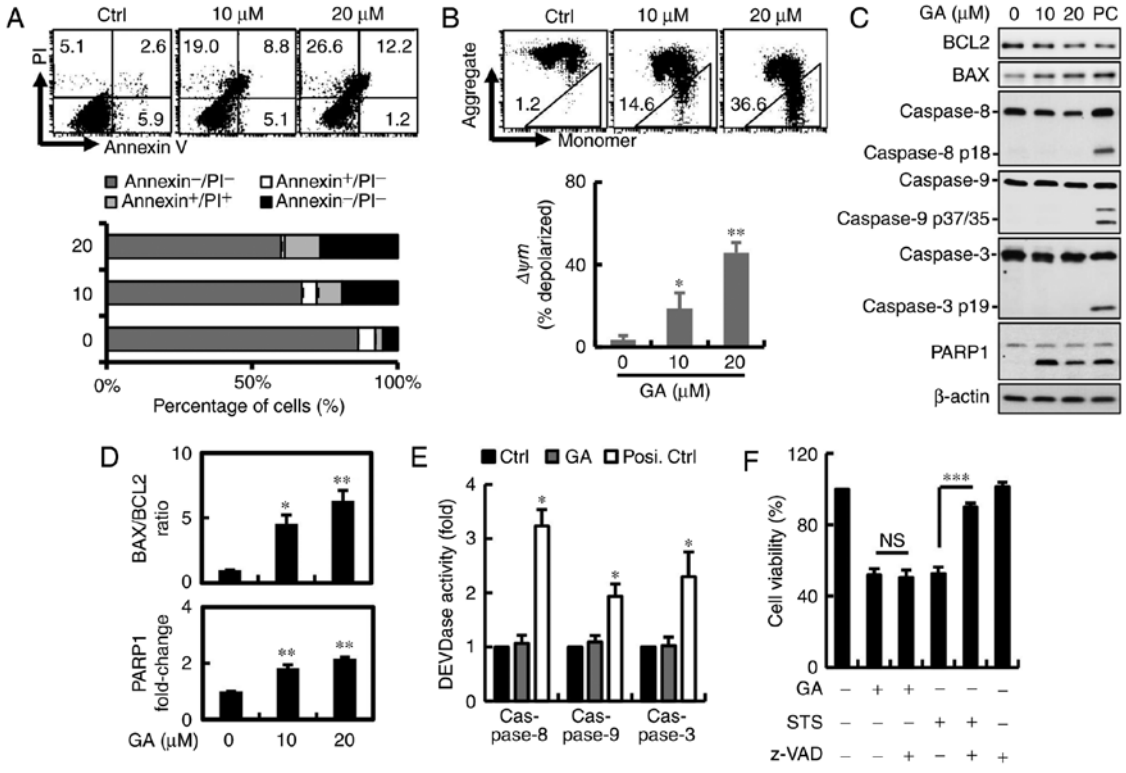

Figure 3. GA induces caspase-independent cell death in MDA-MB-231 cells. (A) Cells were treated with GA for 24 h, and cell death was examined by Annexin V/PI staining followed by flow cytometric analysis. (B) JC-1 disaggregation representing the loss of mitochondrial membrane potential was measured after cells were treated with the indicated concentrations of GA for 24 h. (C and D) Cells were treated with GA for 24 h and detected by immunoblotting. Cells cultured in 0.3 mM H_2O_2 for 4 h served as a positive control. (E) MDA-MB-231 cells were treated with GA and analyzed for caspase activity by the expression of caspase-8, -9 and -3. Cells treated with H_2O_2 for caspase-8 and staurosporine (STS) for caspase-9 and -3 served as the positive control, respectively. (F) Cells were pretreated with z-VAD (50 mM) for 1 h, followed by GA treatment for 24 h prior to CCK-8 assay. *P<0.05, **P<0.01 and ***P<0.001. GA, glycyrrhizic acid; Posi. Ctrl, positive control; STS, staurosporine.

viability was observed after inhibitor pre-treatment in the MDA-MB-231 cells, indicating that GA induced cell death in a caspase-independent manner (Fig. 3F).

Roles of apoptosis-inducing factor (AIF) proteins in GA-induced MDA-MB-231 cell death. To further investigate the cellular mechanism of GA-induced cell death, the protein levels of AIF were detected. AIF is a FAD-dependent oxidoreductase that has a vital role in oxidative phosphorylation and is independent of the caspase pathway. We investigated whether the translocation of AIF occurred in the GA-induced cell death of MDA-MB-231 cells. As shown in Fig. 4A and B, addition of GA resulted in a significant increase in overlap coefficient between nuclear AIF. AIF translocation occurred and subsequently appeared in the nuclear fraction of MDA-MB-231 cells treated with GA for 24 h. We also confirmed and quantified the cellular distribution of AIF. Immunoblotting revealed that AIF mostly resided in the mitochondria of the cancer cells (Fig. 4C). To investigate whether the AIF pathway is involved in the GA-induced cell death, we introduced NPM, an inhibitor that blocks AIF activation, before GA treatment. The results showed that NPM combined with GA had a significant increased on the expression of AIF and PARP1 (Fig. 4D). After the treatment of NPM, JC-1 gathered in the mitochondrial matrix and produced red fluorescence (Fig. 4E). As shown in the results of flow cytometry, GA caused a dramatic reduction in red fluorescence which indicated a loss of mitochondrial membrane potential (ΔΨm) and damage of mitochondria in the MDA-MB-231 cells (Fig. 4F). The ratio of red and green fluorescence represented the level of depolarization in mitochondria: NPM protected MDA-MB-231 cells against the damage caused by GA treatment (Fig. 4G). Moreover, there was increased cell viability after treatment with NPM, indicating that AIF may be the major factor involved in GA-induced cell death (Fig. 4H). Furthermore, NAC treatment also blocked the GA-induced AIF translocation to the nucleus, suggesting that ROS may be the regulator involved in this process (Fig. 4I).

Autophagy and ROS are involved in GA-mediated cell death. Autophagic protein LC-3 is a component of double-membrane vesicle formation into autophagosomes. To explore whether autophagy was involved in GA-induced cell death, the fluorescence expression was utilized. A large number of bubbles were observed in the GA-exposed cells after 24 h (Fig. 5A). Moreover, a number of autophagosomes or lysosomes containing segregated were observed in the GA-treated cells. Conversion from cytosolic LC3-I to LC3-II, the membrane-binding form, was analyzed by western blotting. The protein expression of LC3-II was significantly increased in the MDA-MB-231 breast cancer cells and p62 was downregulated, which is one of the selective substrates for autophagy. These results suggested that AIF and LC3-II may be involved in GA-induced autophagy (Fig. 5B and C). Autophagy is a major process of organelle and protein degradation. An increasing number of studies have shown that autophagy may be a new target for anticancer therapy. To further confirm

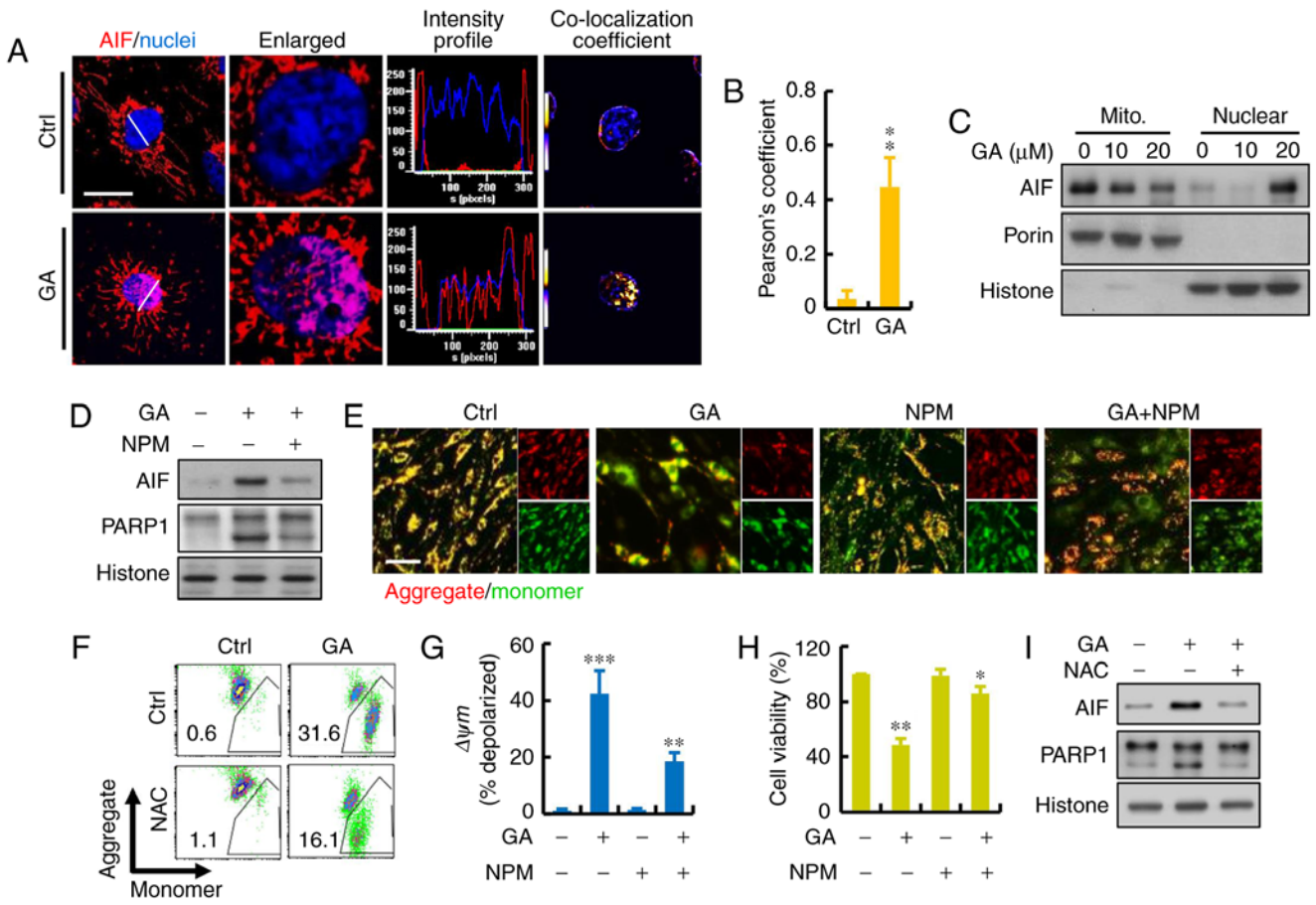

Figure 4. Role of AIF protein in GA-induced MDA-MB-231 cell death. (A) Representative immunofluorescence of AIF (red) and nuclei (blue) using DAPI staining. Calculated and quantification of Pearson's co-localization in the enlarged images, the overlapping of the fluorescence (purple) increased in GA-treated cells. Histograms demonstrate the fluorescence intensity profiles along the lines indicated in the upper row images. Scare bar, 10 μm. (B) Calculated and quantification of Pearson's co-localization coefficients between DAPI and AIF for each group. The coefficients were generated using ImageJ software. (C) AIF release, revealed by western blot analysis in cytosolic and nuclear fractions, was detected in GA-treated breast cancer cells. (D) MDA-MB-231 cell death induced by GA in the presence or absence of AIF inhibitor N-phenylmaleimide (NPM) as measured by immunoblotting. (E) MMP was measured using JC-1 fluorescence imaging in MDA-MB-231 cells. The JC-1 monomer was represented by green fluorescence, the JC-1 aggregate image was represented by red fluorescence, and the merged images were the combined of the green and red images. Control cells showed strong aggregated red fluorescence indicative of normal membrane potential. Scare bar, 100 μm. (F and G) Change in MMP in GA-pretreated MDA-MB-231 cells by flow cytometry. Fluorescence intensity shifted from the higher level to the lower one indicating the loss of MMP. Mitochondrial depolarization is indicated by an increase in the red fluorescence intensity ratio. (H) MDA-MB-231 cell death induced by GA in the presence or absence of AIF inhibitor NPM measured by CCK-8 assay. (I) MDA-MB-231 cell death induced by GA in the presence or absence of ROS inhibitor NAC as measured by immunoblotting; *P<0.05, **P<0.01 and ***P<0.001. GA, glycyrrhizic acid; NAC, *N*-acetyl-cysteine; NPM, *N*-phenylmaleimide.

that autophagy was involved in GA-induced cell death, 2 mM 3 methylamphetamine (3MA), an autophagy blocker that inhibits PI3K class III protein, was added. After addition of 3MA, the increase in LC3 was significantly inhibited compared with the control cells (Fig. 5D). Considering all of the above results, we conclude that GA-induced cell death in MDA-MB-231 cells was mainly due to autophagy. Moreover, there was increased in cell viability after treatment with 3MA, indicating that autophagy may be the major factor involved in GA-induced cell death (Fig. 5E). We further determined the involvement of ROS in GA-induced autophagy, and protein expression of associated signaling molecules (Fig. 5F). NAC reversed the effects of GA on protein expression of LC3 and P62. However, treatment with AIF inhibitor NPM showed no significant effects (Fig. 5G). These results suggested that the anticancer effects of GA on breast cancer cells were mediated by ROS-dependent mitochondrial dysfunction with the involvement of AIF and LC3 signaling pathway.

Discussion

The present study demonstrated that glycyrrhizic acid (GA), the main component of licorice root extracts, is cytotoxic to human breast cancer cell line MDA-MB-231. This effect appears to involve promotion of apoptosis, autophagy and ROS generation via mitochondria. A recent study showed that GA caused a dose-dependent activation of NF-κB as well as ROS generation in HepG2 cells (29). In contract, Thirugnanam *et al* reported that the GA-induced apoptosis in prostate cancer cells was dependent of caspase-3 activation (26). Additional evidence shows that DNA damage-inducing agents trigger caspase-independent apoptosis in various cancer cell lines (23,24). The present study using MDA-MB-231 cells showed that caspase activity was not required for GA-induced apoptosis. zVAD-fmk did not suppress GA-induced apoptosis. Moreover, GA did not induce caspase activation (Fig. 3C). In the present study, our results suggest that GA-induced

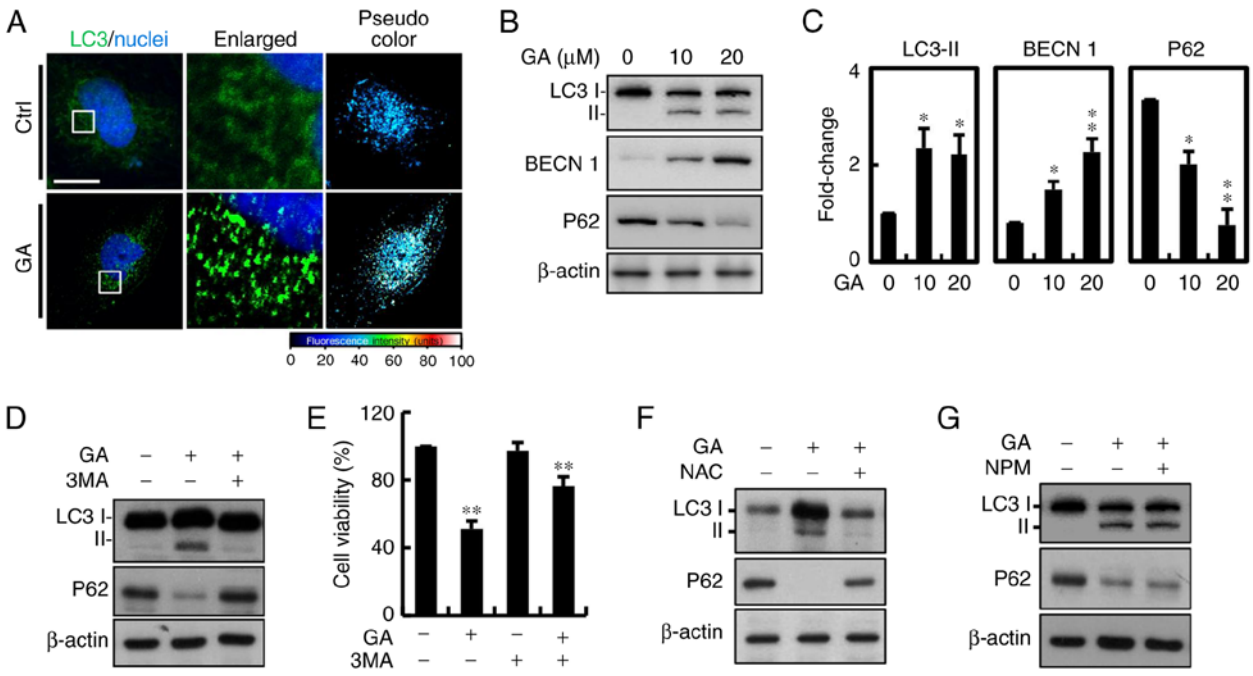

Figure 5. Effects of LC3 protein in GA-induced MDA-MB-231 autophagy. (A) Cells were incubated with GA for 24 h. The punctate structure was evaluated by confocal microscopy. The pseudo-color image shows the formation of autophagic vesicles in cells after treatment for 24 h with GA. Scare bar, 10 μm. (B) The protein expression of autophagic protein LC3, BECN 1 and p62 was measured by western blotting. (C) The protein expression levels were normalized to β-actin and expressed as the fold change to the respective control. (D and E) Cells were pretreated with 3MA (1 M), followed by GA treatment for 24 h prior to immunoblotting analysis and cell survival assay. (F and G) MDA-MB-231 cell death induced by GA in the presence or absence of ROS and AIF inhibitor as measured by immunoblotting. *P<0.05 and **P<0.01. GA, glycyrrhizic acid; NAC, *N*-acetyl-cysteine; NPM, *N*-phenylmaleimide; 3MA, 3 methyladenine.

apoptosis in MDA-MB-231 cells is mediated by a caspase-independent mechanism.

Autophagy or autophagocytosis is a metabolic process involving degradation of cellular components by lysosomes that responds to metabolic stress (30,31). This tightly regulated process helps cells maintain balance and subsequent recycling of cellular organelles and proteins. It is a key mechanism by which starving cells allocate nutrients away from unnecessary processes (32). This mechanism is also associated with progression of certain diseases such as atherosclerosis, neurodegenerative disease and cancers. The two major processes involved are Atg-regulated and chaperone-mediated autophagy (33). Microphagy sequesters damaged organelles other than proteins in a double-membrane autophagosome. Autophagosomes derived from the elongation of small membrane structures are known as autophagosome precursors. The outer membrane of the autophagosome fuses with a lysosome in the cytoplasm to form an autolysosome, in which cell contents undergo acidic degradation (34,35).

As already mentioned earlier, PARP1 belongs to a family of nuclear enzymes, modulating DNA repair, transcriptional regulation, chromatin modification and genomic stability through polyADP-ribosylation (36,37). PARP1 activation leads to ATP depletion, thereby inducing necrosis and apoptosis (38). However, PARP1 can be degraded through multiple downstream proteins, including DNA-dependent protein kinase, ubiquitination and hydrolysis via the proteasome or by the caspase pathway (39). Notably, PARP1 activation interfaces with signalling pathways known to promote autophagy (40). It is well documented that GA-induced cancer cell apoptosis occurs through a mitochondrial pathway. We also observed that GA decreased the levels of $\Delta\Psi$m in MDA-MB-231 cells (Fig. 3B) in a dose-dependent manner. Furthermore, upregulation of BAX, reduction of mitochondrial membrane potentials, enhancement of AIF and LC3 expression, and activation of autophagy were observed in the present study.

In turn, LC3 and AIF activation led to DNA damage, and eventually, induction of autophagic cell death. DNA damage was found in MDA-MB-231 cells after treatment with GA, and downregulation of PARP1 inhibited DNA synthesis and repair; thus, enhanced cytotoxicity through inhibition of DNA repair processes is another possible mechanism explaining the cytotoxic effect of GA. In addition, the greatly increased level of LC3 protein may have contributed to autophagic cell death in the MDA-MB-231 breast cancer cells and reduced cell survival even over long-term treatment. Moreover, autophagosomes were observed through LC3 staining, which may have been activated by excess ROS production in the GA-treated cells. To explore the molecular mechanism of autophagy in GA-induced dell death, an inhibitor of autophagy, 3MA, was added. 3MA partially reversed conversion of LC3, corroborating that autophagy was involved in the GA-induced cell death. These results confirmed the hypothesis that mitochondrial dysfunction occurred via facilitation of apoptosis and autophagy potentially regulated by increased ROS levels in GA-treated breast cancer cells. Based on the antitumor activity profiles of GA treatment *in vitro* and the absence of cytotoxicity, we believe that GA has strong therapeutic value for use against breast cancers.

In conclusion, the present study demonstrated that GA induced apoptotic and autophagic cell death, and inhibited cell growth *in vitro* in breast adenocarcinoma MDA-MB-231 cells. We conclude that GA-induced mitochondrial apoptosis and

autophagy were mainly caused by AIF and LC-3. Our findings suggest that GA warrants further investigation as a promising complementary therapeutic drug for the treatment of human breast cancer.

Acknowledgements

The present study was funded by grants (103-2314-B-442-002-MY3) from the Ministry of Science and Technology, Taiwan, and RB15001 and RB16001 from Show Chwan Memorial Hospital, Taiwan.

References

1. Ertas IE, Sayhan S, Karagoz G and Yildirim Y: Signet-ring cell carcinoma of the breast with uterine metastasis treated with extensive cytoreductive surgery: A case report and brief review of the literature. J Obstet Gynaecol Res 38: 948-952, 2012.
2. Novakovic S, Hocevar M, Zgajnar J, Besic N and Stegel V: Detection of telomerase RNA in the plasma of patients with breast cancer, malignant melanoma or thyroid cancer. Oncol Rep 11: 245-252, 2004.
3. A new therapy standard in metastatic breast cancer - gemzar/paclitaxel. Longer survival by optimized combination therapy. Krankenpfl J 42: 235, 2004 (In German).
4. Engel J, Ludwig MS, Schubert-Fritschle G, Tretter W and Hölzel D: Cancer prevention and the contribution of cancer registries. J Cancer Res Clin Oncol 127: 331-339, 2001.
5. Stickeler E: Prognostic and predictive markers for Treatment Decisions in Early Breast Cancer. Breast Care 6: 193-198, 2011.
6. Andergassen U, Kölbl AC, Mumm JN, Mahner S and Jeschke U: Triple-negative breast cancer: New therapeutic options via signalling transduction cascades. Oncol Rep 37: 3055-3060, 2017.
7. Rakha EA, El-Sayed ME, Green AR, Lee AH, Robertson JF and Ellis IO: Prognostic markers in triple-negative breast cancer. Cancer 109: 25-32, 2007.
8. Hoge AF, Asal N, Owen W and Anderson P: Histologic and staging classification of breast cancer: Implications for therapy. South Med J 75: 1329-1334, 1982.
9. Bazel S, Ferry K, Shoarinejad F, Laurykleintop L, Lange M, Tachovsky T, Longo S, Tucker S and Alhadeff J: Analysis of breast-tissue cathepsin-d isoforms from patients with breast-cancer, benign breast disease and from normal controls. Int J Oncol 5: 847-853, 1994.
10. Wu S, Dahut WL and Gulley JL: The use of bisphosphonates in cancer patients. Acta Oncol 46: 581-591, 2007.
11. Sopkova V and Mechl Z: Cisplatin (platidiame) in the treatment of patients with disseminated breast cancer. Vopr Onkol 32: 36-38, 1986 (In Russian).
12. Kolacinska A, Chalubinska J, Zawlik I, Szymanska B, Borowska-Garganisz E, Nowik M, Fendler W, Kubiak R, Pawlowska Z, Morawiec Z, *et al*: Apoptosis-, proliferation, immune function-, and drug resistance-related genes in ER positive, HER2 positive and triple negative breast cancer. Neoplasma 59: 424-432, 2012.
13. Conley SJ, Gheordunescu E, Kakarala P, Newman B, Korkaya H, Heath AN, Clouthier SG and Wicha MS: Antiangiogenic agents increase breast cancer stem cells via the generation of tumor hypoxia. Proc Natl Acad Sci USA 109: 2784-2789, 2012.
14. Shimoyama S: Unraveling trastuzumab and lapatinib inefficiency in gastric cancer: Future steps (Review). Mol Clin Oncol 2: 175-181, 2014.
15. Noguchi E, Kamio T, Kamio H, Miura H, Tamaki M, Nishizawa M, Aoyama K, Oochi T and Kameoka S: Efficacy of lapatinib monotherapy on occult breast cancer presenting with cutaneous metastases: A case report. Oncol Lett 8: 2448-2452, 2014.
16. Ming LJ and Yin AC: Therapeutic effects of glycyrrhizic acid. Nat Prod Commun 8: 415-418, 2013.
17. Huang RY, Chu YL, Jiang ZB, Chen XM, Zhang X and Zeng X: Glycyrrhizin suppresses lung adenocarcinoma cell growth through inhibition of thromboxane synthase. Cell Physiol Biochem 33: 375-388, 2014.
18. He SQ, Gao M, Fu YF and Zhang YN: Glycyrrhizic acid inhibits leukemia cell growth and migration via blocking AKT/mTOR/STAT3 signaling. Int J Clin Exp Pathol 8: 5175-5181, 2015.
19. Afnan Q, Kaiser PJ, Rafiq RA, Nazir LA, Bhushan S, Bhardwaj SC, Sandhir R and Tasduq SA: Glycyrrhizic acid prevents ultraviolet-B-induced photodamage: A role for mitogen-activated protein kinases, nuclear factor kappa B and mitochondrial apoptotic pathway. Exp Dermatol 25: 440-446, 2016.
20. Park JM, Park SH, Hong KS, Han YM, Jang SH, Kim EH and Hahm KB: Special licorice extracts containing lowered glycyrrhizin and enhanced licochalcone A prevented *Helicobacter pylori*-initiated, salt diet-promoted gastric tumorigenesis. Helicobacter 19: 221-236, 2014.
21. Li S, Zhu JH, Cao LP, Sun Q, Liu HD, Li WD, Li JS and Hang CH: Growth inhibitory in vitro effects of glycyrrhizic acid in U251 glioblastoma cell line. Neurol Sci 35: 1115-1120, 2014.
22. Cao B, Li J, Zhou X, Juan J, Han K, Zhang Z, Kong Y, Wang J and Mao X: Clioquinol induces pro-death autophagy in leukemia and myeloma cells by disrupting the mTOR signaling pathway. Sci Rep 4: 5749, 2014.
23. Nurdin SU, Le Leu RK, Young GP, Stangoulis JC, Christophersen CT and Abbott CA: Analysis of the anti-cancer effects of cincau extract (*Premna oblongifolia* Merr) and other types of non-digestible fibre using faecal fermentation supernatants and Caco-2 cells as a model of the human colon. Nutrients 9: pii: E355, 2017.
24. Pang L, Zhao X, Liu W, Deng J, Tan X and Qiu L: Anticancer effect of ursodeoxycholic acid in human oral squamous carcinoma HSC-3 cells through the caspases. Nutrients 7: 3200-3218, 2015.
25. Chueh FS, Hsiao YT, Chang SJ, Wu PP, Yang JS, Lin JJ, Chung JG and Lai TY: Glycyrrhizic acid induces apoptosis in WEHI-3 mouse leukemia cells through the caspase- and mitochondria-dependent pathways. Oncol Rep 28: 2069-2076, 2012.
26. Thirugnanam S, Xu L, Ramaswamy K and Gnanasekar M: Glycyrrhizin induces apoptosis in prostate cancer cell lines DU-145 and LNCaP. Oncol Rep 20: 1387-1392, 2008.
27. Zafar R and Neerja : Momordica charantia - a review. Hamdard Med 34: 49-61, 1991.
28. Li CJ, Chu CY, Huang LH, Wang MH, Sheu LF, Yeh JI and Hsu HY: Synergistic anticancer activity of triptolide combined with cisplatin enhances apoptosis in gastric cancer in vitro and in vivo. Cancer Lett 319: 203-213, 2012.
29. Hsiang CY, Lin LJ, Kao ST, Lo HY, Chou ST and Ho TY: Glycyrrhizin, silymarin, and ursodeoxycholic acid regulate a common hepatoprotective pathway in HepG2 cells. Phytomedicine 22: 768-777, 2015.
30. Tu YF, Kaipparettu BA, Ma Y and Wong LJ: Mitochondria of highly metastatic breast cancer cell line MDA-MB-231 exhibits increased autophagic properties. Biochim Biophys Acta 1807: 1125-1132, 2011.
31. Shen M, Duan WM, Wu MY, Wang WJ, Liu L, Xu MD, Zhu J, Li DM, Gui Q, Lian L, *et al*: Participation of autophagy in the cytotoxicity against breast cancer cells by cisplatin. Oncol Rep 34: 359-367, 2015.
32. Abounit K, Scarabelli TM and McCauley RB: Autophagy in mammalian cells. World J Biol Chem 3: 1-6, 2012.
33. Kaushik S, Kiffin R and Cuervo AM: Chaperone-mediated autophagy and aging: A novel regulatory role of lipids revealed. Autophagy 3: 387-389, 2007.
34. Richard V, Kindt N and Saussez S: Macrophage migration inhibitory factor involvement in breast cancer (Review). Int J Oncol 47: 1627-1633, 2015.
35. Richard V, Kindt N, Decaestecker C, Gabius HJ, Laurent G, Noël JC and Saussez S: Involvement of macrophage migration inhibitory factor and its receptor (CD74) in human breast cancer. Oncol Rep 32: 523-529, 2014.
36. Nikoletopoulou V, Markaki M, Palikaras K and Tavernarakis N: Crosstalk between apoptosis, necrosis and autophagy. Biochim Biophys Acta 1833: 3448-3459, 2013.
37. Krishnakumar R and Kraus WL: The PARP side of the nucleus: Molecular actions, physiological outcomes, and clinical targets. Mol Cell 39: 8-24, 2010.
38. Gerö D, Szoleczky P, Chatzianastasiou A, Papapetropoulos A and Szabo C: Modulation of poly(ADP-ribose) polymerase-1 (PARP-1)-mediated oxidative cell injury by ring finger protein 146 (RNF146) in cardiac myocytes. Mol Med 20: 313-328, 2014.
39. Wang Z, Wang F, Tang T and Guo C: The role of PARP1 in the DNA damage response and its application in tumor therapy. Front Med 6: 156-164, 2012.
40. Arun B, Akar U, Gutierrez-Barrera AM, Hortobagyi GN and Ozpolat B: The PARP inhibitor AZD2281 (Olaparib) induces autophagy/mitophagy in *BRCA1* and *BRCA2* mutant breast cancer cells. Int J Oncol 47: 262-268, 2015.